

# Oxidation of Metallic Nanoparticles

A. Auge,<sup>1,\*</sup> A. Weddemann, B. Vogel, F. Wittbracht, and A. Hütten

<sup>1</sup> Bielefeld University, Department of Physics, Thin Films and Physics of Nanostructures

\*Corresponding author: Bielefeld University, Universitätsstr. 25, 33615 Bielefeld,

email: aauge@physik.uni-bielefeld.de

**Abstract:** The oxidation behavior of metallic nanoparticles is investigated in respect to material parameters like Mott potential, defects on the microstructure and oxide volume increase per ionic defect. An emphasis is laid on magnetic nanoparticles where the degree of oxidation can be measured via the reduction of the magnetic moment.

**Keywords:** Nanoparticle, Oxidation, Level Set Method

## 1. Introduction

Metallic nanoparticles have become important in many fields like biotechnology, chemistry and physics.<sup>1</sup> One important example in this area is magnetic nanoparticles.<sup>2</sup> For many applications it is mandatory that magnetic properties of the nanoparticles are stable for a long time.<sup>3</sup> The reduction of the magnetic moment of the particle is due to oxidation of the magnetic material like Fe or Co. The oxidation process in nanoparticles can be described by a model introduced by Cabrera and Mott<sup>4</sup> that was further improved by Fromhold.<sup>5</sup>

In this work the simulation of oxidation is realized via a Level set approach modeling the evolution of the metal-oxide interface. This offers the possibility to investigate the growth of the oxide layer in dependence of the microstructure that is introduced by grain or core-shell structures.

## 2. Theoretical model

In general the growth of oxide films is controlled by diffusion of ions and electrons under the influence of gradients of their concentration and self generated electric fields. In the case of nanoparticles, the electric field is very strong and hence its influence is significant. A generic model describing the kinetics of oxide growth under the effect of this electric field was introduced by Cabrera and Mott.<sup>4</sup> An improved

model was developed by Fromhold et al.<sup>5</sup> According to the latter model the oxide growth can be divided into the following steps:

1. Dissociative adsorption of oxygen from the gas phase to the surface of the particle
2. Oxidation of surface metal atoms
3. Ionization of adsorbed oxygen atoms and metal ions at the metal-oxide interface
4. Build up of a self generated electric field
5. Incorporation of metal ions into the oxide layer at the metal-oxide interface
6. Diffusion of metal ions within the oxide layer
7. Reaction of metal ions with oxygen ions to form metal oxide

For geometries below 200 nm the electric field is the driving force of the oxidation, and hence its origin and strength is of major significance. The mechanism of ionization depends on the ambient temperature, the work-function of the oxidizing metal and the oxide thickness. For low temperatures the ionization occurs via electron tunneling from the metal-oxide interface to the adsorbed oxygen. Considering the energy level diagram in Fig. 1, the driving force of the tunneling can be easily understood.

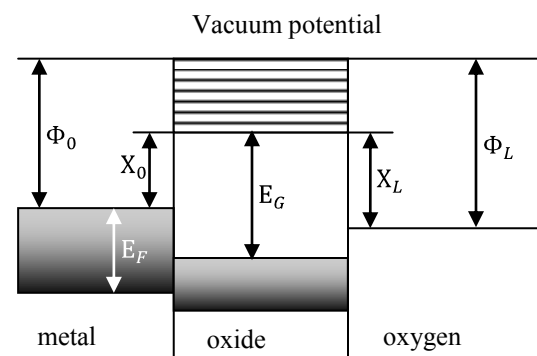


**FIG. 1:** Energy level diagram of the metal-oxide-oxygen system. The tunneling process stops as soon as the potentials  $X_L$  and  $X_0$  reach equilibrium

Tunneling occurs due to the potential difference of the metal  $\Phi_0$  and the oxygen  $\Phi_L$  until the electric field  $E_0$  of the ions is as strong as the potential difference

$$V_m = \phi_0 - \phi_L = E_0 L \quad (1)$$

where  $V_m$  the so called Mott potential and  $L$  the oxide thickness. For higher temperatures thermal emission of electrons is also important which however is not considered here. The tunnel current  $J_e$  is given by the following expression<sup>5</sup>

$$J_e = \{8\pi\hbar L(t)^2\}^{-1} \{2\chi_0 + eE_0 L(t)\} \cdot \exp\left\{-2\sqrt{m_e \hbar^{-1} L(t)} \sqrt{2\chi_0 + eE_0 L(t)}\right\} - \{2\chi_L - eE_0 L(t)\} \cdot \exp\left\{-2\sqrt{m_e \hbar^{-1} L(t)} \sqrt{2\chi_L - eE_0 L(t)}\right\} \quad (2)$$

with  $\hbar$  the Planck constant and  $m_e$  the electron mass. The ionic diffusion current in the absence of space charge effects is given in the steady state approximation by<sup>5</sup>

$$J_i = 4av \exp\left(-\frac{W}{kt}\right) \sinh(Z_i E_0 a / kt) \cdot \{C_i(L) - C_i(0) \exp\left[\frac{Z_i e E_0 L(t)}{kt}\right]\} / \left\{1 - \exp\left[\frac{Z_i e E_0 L(t)}{kt}\right]\right\} \quad (3)$$

The parameters  $C_i(L)$  and  $C_i(0)$  are the bulk defect concentrations of the diffusing ionic species at the oxide-oxygen and at the metal oxide interface, respectively.  $E_0$  is the surface charge field in the oxide,  $e$  the elementary charge,  $Z_i e$  the effective charge of the transported ionic species,  $a$  the lattice constant,  $k$  the Boltzmann constant,  $T$  the temperature and  $W$  the thermal activation energy for ionic motion. The assumption that the steady state currents are equal in magnitude but opposite in sign leads to the following equation<sup>5</sup>

$$q_i J_i + q_e J_e = 0 \quad (4)$$

This condition is used to determine the self generated electric field in the oxide layer. The growth of the oxide layer is then given by<sup>5</sup>

$$\frac{dL}{dt} = R_c J_i \quad (5)$$

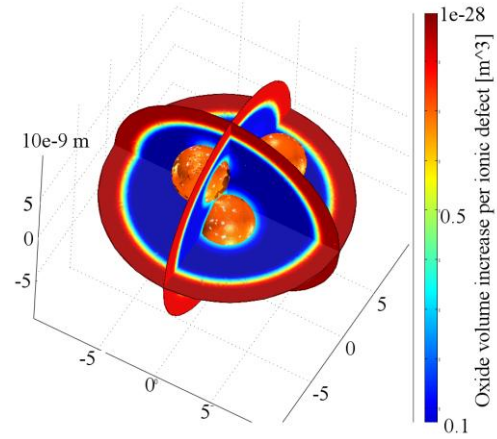


**FIG. 2** Nanoparticle with different oxide volume increase rates. Grains are colored in orange. The shell and core are shown as red and blue regions, respectively.

where  $R_c$  denotes the oxide volume increase per transported ionic defect.

### 3. Simulation model

For this simulation model the nanoparticle is approximated by a sphere of radius  $R$  and oxide layer thickness  $L$ . The growth of the oxide layer is implemented via a Level set approach.<sup>7</sup> This method is capable of describing the motion of surfaces and often used in multiphase flows. Here it is used to track the motion of the metal-oxide interface.

The basic idea of the Level set method is to express a surface in an implicit form, as the zero level set or isophote of a higher dimensional function  $\Phi(\vec{r})$  and then trace the deformation of the surface by means of deformation of this embedding function. Generally, for a given domain  $\Omega$  with smooth boundary, we assume the existence of an implicit function  $\Phi(\vec{r})$  which satisfies

$$\begin{cases} \Phi(\vec{r}) > 0 & \vec{r} \in \Omega^+ (\text{oxide}) \\ \Phi(\vec{r}) = 0 & \vec{r} \in \partial\Omega (\text{interface}) \\ \Phi(\vec{r}) < 0 & \vec{r} \in \Omega^- (\text{metal}) \end{cases}$$

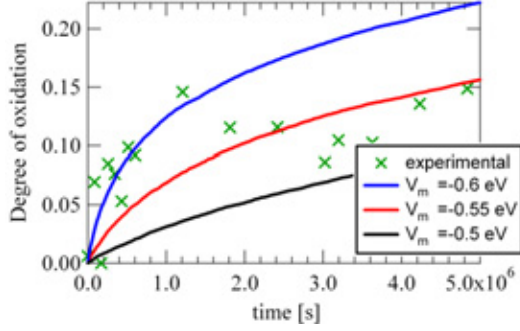


**FIG. 3:** Comparison between experimental data for the oxidation of Co nanoparticles with  $R = 3.8 \pm 0.08$  nm and simulation results for different values of the Mott potential. All other parameters are given in Tab.1.

The dynamic evolution of the Level set function follows the convection diffusion equation

$$\frac{\partial \Phi(\vec{r})}{\partial t} + V_n \nabla \Phi(\vec{r}) + D \Delta \Phi(\vec{r}) = 0 \quad (5)$$

where  $V_n$  the normal velocity of the moving boundary and  $D$  is the diffusion coefficient. In the investigated systems diffusion is **only** introduced to maintain numerical stability. Equation (5) defines the motion of the zero level set  $\Phi(\vec{r}) = 0$ . As an initial condition, we set

$$\Phi(\vec{r}) = R - \sqrt{x^2 + y^2 + z^2} \quad (6)$$

This is a signed distance function, and therefore, has the advantage that  $|\nabla \Phi(\vec{r})| = 1$  for most of the domain except at the center where certain partial derivatives are not defined. The normal vector of the implicit surface is calculated via  $\vec{N} = \nabla \Phi$ . The growth of the oxide layer and thus the normal velocity  $V_n$  is given by equation (5). It is implemented in the following way

$$\frac{\partial \Phi(\vec{r})}{\partial t} + R c J_i \vec{N} \nabla \Phi(\vec{r}) + D \Delta \Phi(\vec{r}) = 0 \quad (7)$$

The ionic current  $J_i$  is determined for each time step using equation (4). For this the distance  $L$  has to be calculated which is done via linear regression.

$$L = R - |\vec{r} - \Phi(\vec{r}) \vec{N}| \quad (8)$$

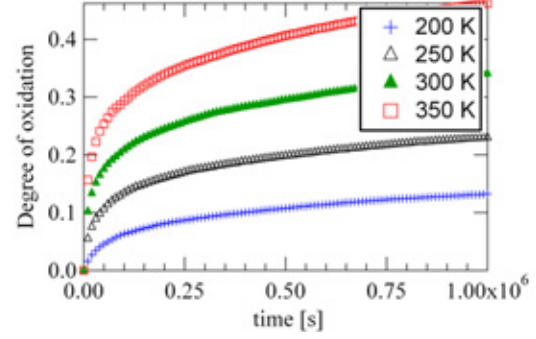


**FIG. 4:** Oxidation in dependence of temperature of a nanoparticle with  $R = 5$  nm and an initial oxide layer of 1nm. All other parameters are given in Tab. 1.

It is also possible to implement further details like structural defects, grain structures or core shell nanoparticles by varying the oxide volume by an increase of  $R_c$  on the nanoparticle domain. This is shown in Fig. 2. In this example the shell has a high oxide volume increase per ionic defect. Grains within the material are presented as orange subdomains inside the core.

#### 4. Simulation results

To verify the simulation model, experimental data are compared to calculated oxidation curves. For all simulations an initial oxide thickness of 1 nm is assumed. The oxidation degree given neglects this initial oxidation. This coincides with experimental conditions, where the measurements start after a certain oxidation time. In Fig. 3 experimental data of Co nanoparticles with a mean radius of  $R = 3.8 \pm 0.08$  nm and simulation results are shown. The nanoparticles oxidized at room temperature and the loss of magnetization is measured via an Alternating Gradient Magnetometer. To calculate the loss of magnetization the degree of oxidation is used. The simulation fits well to the experimental data if a Mott potential of  $V_m = -0.55 \pm 0.05$  eV and remaining parameters according to Tab. 1 are chosen.

Furthermore, the oxidation of nanoparticles in dependence of temperature and the oxygen work function are investigated. In Fig. 4 oxidation curves for different temperatures is shown. All curves show a rapid increase of oxidation followed by a slow linear increase. For

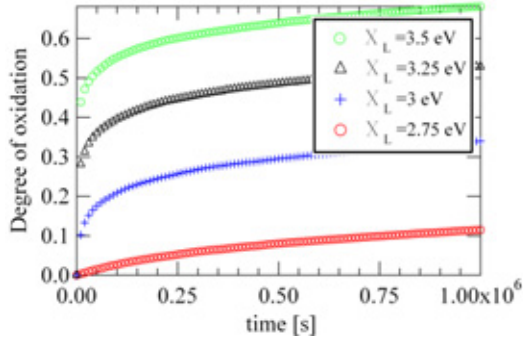


**FIG. 5:** Oxidation in dependence of the oxide work function of a nanoparticle with  $R = 5\text{nm}$  and an initial oxide layer of  $1\text{ nm}$ . All other parameters are given in Tab. 1.

rising temperature, the initial fast oxidation increases rapidly. The slow increase is also affected by a change of slope. The change of the oxidation rate is due to the increase of the ionic current, which is exponentially affected by the temperature.

In Fig. 5 the oxidation in dependence of the oxygen work function is shown. For  $X_L > 2.75\text{ eV}$  the initial fast oxidation is visible. For  $X_L = 2.75\text{ eV}$  the growth shows a linear behavior. This can be attributed to growth kinetics limited by the electron current. In Fig. 6 the effect of different growth regions, which is possible with the Level set method, is shown. Deformations of the metal-oxide interface are visible where the growth rate is enhanced.

## 5. Summary and Outlook

In this work a Level set based method is introduced to model the oxidation dynamics of metallic nanoparticles. A comparison between experimental data from the oxidation of Co nanoparticles shows good agreement with the simulations. It has also been shown, that it is possible with the proposed approach to model different regions of growth within the nanoparticle. For the future, further studies on the influence of the latter are planned.

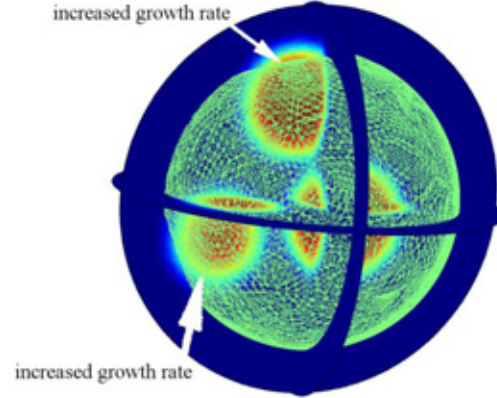


**FIG. 6:** Regions with different growth rates of nanoparticle as well as an oxide-metal interface (green layer) are shown. A distortion of the interface is visible at the areas with increased oxide growth rate.

## 6. Appendix

Symbol	Definition	Value
$X_0$	Metal oxide work function (eV)	2
$X_L$	$O^-$ work function (eV)	2.5
$V_m$	Mott potential (eV)	-0.5
$T$	Temperature (K)	300
$2a$	Ionic jump distance ( $\text{\AA}$ )	4.25
$C_i(0)$	Ionic defect concentration at metal oxide interface ( $\text{cm}^{-3}$ )	$10^{18}$
$C_i(L)$	Ionic defect concentration at oxide oxygen interface ( $\text{cm}^{-3}$ )	$10^{15}$
$R_c$	Oxide volume increase per transported ionic defect ( $\text{\AA}^3$ )	19.19

**Table 1:** Parameters used for simulations

## References

- <sup>1</sup>J. Blackman, *Metallic Nanoparticles*, Elsevier (2009)
- <sup>2</sup>S. P. Gubin, *Magnetic Nanoparticles*, Wiley-VCH (2009)
- <sup>3</sup>G. A. Niklasson, R. Karmhag, *Surface Science* **532–535**, 324–327 (2003)
- <sup>4</sup>N. Cabrera et al., *Rept. Progr.Phys.* **12**, 163 (1949)
- <sup>5</sup>A. T. Fromhold, E.A. Cook, *Phys. Rev.* **158**, 600–612 (1967)
- <sup>6</sup>S. Osher, R. Fedkiw, *Level Set Methods and Dynamic Implicit Surfaces*, Springer (2002)